

# Terrain-Based Localization and Mapping for Autonomous Underwater Vehicles using Particle Filters with Marine Gravity Anomalies

Parth Pasnani\*, Mae L. Seto, Senior Member, IEEE \*\*

\*Dalhousie University, Halifax, NS, Canada (e-mail: [parth.pasnani@dal.ca](mailto:parth.pasnani@dal.ca)).

\*\*Dalhousie University, Halifax, NS, Canada (e-mail: [mae.seto@dal.ca](mailto:mae.seto@dal.ca))

**Abstract:** The feasibility of using prior gravity anomaly measurements that are 1 nautical mile apart for underwater simultaneous localization and mapping is studied. This paper reports on modelling and simulation that investigates relationships between the characteristic anomaly parameters and the requirements for particle filter SLAM solutions. Map anomaly variability parameters suggest the gross likelihood of SLAM success in a map. However, the anomaly parameters that relate to the local anomaly measurement-to-measurement variability (i.e. localization) are better indicators for a SLAM mission's success. The prior gravity anomaly measurements, coupled with the tools developed here, provide guidance to select optimal areas and missions the AUV could transit through towards minimal localization error at the goal location. Follow-on work will exploit the anomaly localization parameter to assist with SLAM path-planning through a vector field histogram approach and then, implement it on an AUV for validation.

© 2018, IFAC (International Federation of Automatic Control) Hosting by Elsevier Ltd. All rights reserved.

**Keywords:** autonomous underwater vehicle, localization, mapping, particle filters, gravity anomalies

## 1. INTRODUCTION

The feasibility of prior gravity anomaly measurements for localization and mapping of autonomous underwater vehicles (AUV), and potentially simultaneous localization and mapping (SLAM) is studied initially through modelling and simulation. With SLAM, the robot creates (or updates) a map and concurrently locates itself within that map. The accuracy of the localization (or map) requires the AUV to re-visit, and correctly associate, previously observed landmarks (features) to reduce the cumulated AUV position error. This data association is the difficult step. Underwater data association challenges stem from a scarcity of distinctive landmarks, no universal positioning system, and underwater communications that is limited in range and bandwidth.

SLAM has been applied to controlled environments and underwater naval countermeasures (Saeedi, et al., 2016) with some success. To fully realize the value of AUVs, the next step is to localize and map at extended ranges and durations without surfacing for a global positioning satellite (GPS), or other, position calibration. Minimal surfacing can be due to stealth requirements or that the AUV is operating under-ice.

Under-ice operation at long ranges imply that positioning aids like GPS and/or surface ships with beacons are inaccessible to AUVs for localization, navigation or mapping. Therefore, terrain-based, or terrain referenced, methods are considered (Melo & Matos, 2017). These techniques exploit natural environmental landmarks or features in the bathymetry

(seabed topography), magnetic field or gravitational field. Bathymetry is measured with multi-beam echo-sounders which measure the seabed geometry from acoustic returns. Magnetometers sense the local Earth's magnetic field. Gravitational fields are measured with gravimeters which sense the vertical acceleration component due to gravity relative to a reference like  $9.81 \text{ m/s}^2$  (hence, 'anomaly'). Additionally, gravity gradiometers sense the local rate of change in Earth's gravitational field. All these sensors have been previously integrated and operated on-board AUVs.

### 1.1 Potentially More Information

Magnetic field features are less reliable landmarks as the AUV operates closer to the poles due to the convergence of magnetic flux lines there. Their measurements are not consistently reproducible starting north of 60 degrees latitude in the Canadian Arctic with some magnetometers. The use of bathymetry measurements with multi-beam sonars and prior maps is widely considered for terrain-based navigation as the world-wide database of digital terrain maps grow (Heath, et al., 2005). However, not all underwater areas are characterized by distinctive bathymetric features.

Bathymetry over most of the ocean can be featureless which challenges underwater localization, navigation and mapping. Digital terrain measurements can be converted to approximate gravity anomaly measurements based on an assumed constant terrain density (Yan, et al., 2014). This assumption means there is no additional information over the bathymetric

geometry however, this approximation is more accessible than gravimeter measurements. The assumption also does not exploit the presence of materials like ore deposits under the seabed which provide distinctive local anomalies. Unlike bathymetry geometry, gravitation anomalies have low and high frequency components which are additional attributes towards a better SLAM solution. There are other inherent advantages to sensing with gravity anomalies.

### 1.2 Other Advantages

Gravity is especially a property of large physical masses like the Earth. Unlike bathymetry, Earth's gravitational field persists and is stable – not easily changing due to natural or manmade activities unless obviously their scale is large. Bathymetry, magnetic fields and other natural and man-made underwater features evolve. This has driven the need for time-varying SLAM (Walcott-Bryant, et al., 2012). Unlike other physical properties sensed underwater, the gravitational field is unevenly distributed with variable features – maybe distinctive enough for SLAM.

Like bathymetric SLAM, if gravitational fields can be used, the AUV would not have to surface to reduce its position error. As well, there are no external emissions that need to be transmitted to, or received by, the AUV and its sensing is a passive self-contained system. The anomaly sensing cannot be detected, interfered with or jammed unlike GPS, radar, sonar or laser. Gravitational field sensing works in all weather and is limited only by the AUV. Depending on the marine area, prior gravity maps from satellite altimetry are available.

### 1.3 Autonomous Underwater Vehicles

AUVs were recognized for their potential to conduct precise, spatially-dense gravity surveys over 25 years ago (Jircitano, et al., 1990). Until recently, AUVs did not have the on-board endurance, navigation solutions or localization necessary.

For ocean science observation, the Woods Hole Oceanographic Institution (WHOI) used human occupied vehicles (HOV) that crawled on the seabed as platforms for marine gravimeter measurements (Kinsey, et al., 2008). However, this did not localize the gravimeter well. Vehicle motions would bias the gravimeter measurements. Using surface ships as gravimeter platforms is another method. Gravimeters have also been used on-board HOV like the WHOI 2-man ALVIN submersible. It was acknowledged that AUVs have advantages over HOVs. The AUV's closed-loop depth control holds depth to within centimeters unlike ships, ALVIN or towed sleds. AUVs also have a separation between their centers of buoyancy and gravity which confers better attitude stability than tethered remotely operated vehicles and HOVs. The attitude stability and precise depth-keeping reduces the vertical vehicle-induced gravitational acceleration. As well, the AUV's submerged endurance and free-swimming

ability to transit long distances make them good platforms for gravity surveys.

There is current work that considers AUVs as platforms for gravity anomaly measurements, localization, and navigation with (Wu, et al., 2010), (Wang, et al., 2017a), (Ishihara, et al., 2015), (Yan, et al., 2014), (Kiselev, et al., 2017) and (Shinohara, et al., 2017) to name a few. (Ishihara, et al., 2015), (Araya, et al., 2015), (Wang, et al., 2016) and (Shinohara, et al., 2017) have integrated gravimeters and/or gradiometers for geological surveys and resource exploration on-board AUVs. Their navigation resolutions ( $\pm 2$  nm) are sufficient for localizing large distributed ore deposits. Is this sufficient for long range AUV localization and mapping?

Gravity-based methods localize the AUV by matching local anomaly measurements against a prior reference map. *Therefore, the gravity-based SLAM feasibility depends on the accuracy and uncertainties of the: AUV navigation solution, gravimeter measurement, reference map, and matching algorithm.* The AUV navigation solution for follow-on validation of this work is a Kearfott T86 INS with a Rowe Doppler velocity log to measure speed-over-ground. This state-of-the-art system has an error of 1% of the along-track distance travelled. This is the navigation solution modelled in the simulations. The best on-board gravimeter measurement is assumed from previous work (Ander, et al. 1999) at  $\pm 1 - 2$  mGal (1 Gal = 1 cm/s<sup>2</sup>). The reference map accuracy is given as 3 – 8 mGal. Unlike approaches that exhaustively search the map to best match the anomaly measurements, SLAM performs the matching through its data association step.

The work here studies the efficacy of AUV SLAM by simulating the use of prior gravitational anomaly maps and on-board measurements. Emphasis is on the matching through data association and the impact of the gravitation terrain on localization (and mapping) accuracy. This has not been studied or reported on for gravitational anomalies.

The rest of this paper is organized as follows. Section 2 describes marine gravity anomaly map characterizations and the AUV localization particle filter developed. Then, Section 3.0 presents the work of this paper to investigate the feasibility and efficacy of SLAM with underwater gravity anomaly and gradient measurements implemented with featureless particle filters. Section 4.0 discusses the results and presents the major findings. Section 5.0 concludes with a few remarks.

## 2. APPROACH AND METHODOLOGY

### 2.1 Marine Gravity Anomaly Measurements

Gravity-aided inertial navigation has been verified in principle through previous work (Wang, et al., 2016) (Wang, et al., 2017b) with a ship-board gravimeter. This yielded valuable data sets with ground truth GPS localization accuracy. The marine gravity anomaly measurements from reference maps

have variability which has been quantified. The hypothesis is that these quantities might provide guidance on the anomaly areas useful for SLAM towards long range localization. These quantities are described next.

## 2.2 Characterizing Prior Gravity Maps

Through the Scripps Institution of Oceanography, geo-referenced gravimeter measurements are available at spatial frequencies of 1 minute  $\times$  1 minute for marine environments. They will be considered geo-referenced landmarks here. A map area of  $m \times n$  points, has gravimeter measurements,  $G$ , at each latitude and longitude in the map. The standard deviation,  $\sigma$ , is these measurements' deviation between points in the map and the mean map anomaly, i.e.:

$$\sigma = \sqrt{\left(\frac{1}{mn-1} \sum_{i=1}^m \sum_{j=1}^n (G(i,j) - \bar{G})^2\right)} \quad (1)$$

such that  $G(i,j)$  is the gravity anomaly at map location  $(i,j)$  and  $\bar{G}$  is the mean map anomaly.  $\sigma$  (larger is better) qualitatively relates to the navigation in the map. Roughness,  $r$ , of the anomaly measurement captures the variation between adjacent points in the map at a finer scale (Wang, et al., 2017a):

$$r_{longitude} = \frac{1}{(m-1)n} \sum_{i=1}^{m-1} \sum_{j=1}^n |G(i,j) - G(i+1,j)|, \\ r_{latitude} = \frac{1}{m(n-1)} \sum_{i=1}^m \sum_{j=1}^{n-1} |G(i,j) - G(i,j+1)| \text{ and} \\ \therefore r = (r_{longitude} + r_{latitude})/2. \quad (2)$$

If  $r$  is insignificant compared to the mapped and on-board measurement uncertainty, it suggests localization difficulty. The macroscopic window standard deviation and microscopic local roughness can be combined into one parameter,  $\Gamma(i,j)$ :

$$S_{long} = [G(i,j) - G(i-k,j)]^2 + [G(i,j) + G(i+k,j)]^2, \\ S_{lat} = [G(i,j) - G(i,j-k)]^2 + [G(i,j) + G(i,j+k)]^2 \text{ and} \\ \therefore \Gamma(i,j,k) = \sqrt{(S_{long} + S_{lat})/4} \quad (3)$$

such that  $\Gamma(i,j,k)$  characterizes the anomaly at point  $O(i,j)$  in the window from an observation  $k$  grid intervals away. The overall characteristic measure of the map is defined as:

$$\Gamma(k) = \sqrt{\left(\frac{1}{mn-1} \sum_{i=1}^m \sum_{j=1}^n \Gamma^2(i,j)\right)}. \quad (4)$$

Only  $k = 1$  to 6 for  $\Gamma(k)$  are considered. They qualitatively relate to the map localization fitness. As per (Wang, et al., 2017a), if  $\Gamma(k = 4, 5, 6) \geq 9.3$  the region may reach its best localization accuracy of  $\sim \pm k_{\max}(\Gamma_k)/2$  nm. Given this nonlinear variability of marine gravity features, featureless landmarks using particle filter SLAM will be used (Barkby, et al., 2011). The next subsection describes what gravity anomaly localization would look like with particle filters.

## 2.3 Particle Filter Analysis

The Rao-Blackwellized particle filter (Barkby, et al., 2011) of size  $N$ , enumerated by  $m$ , propagates each particle through motion model,  $f_t$ , in Eq. (5). The AUV state (position) is  $s_{m,t} = [s_{1,m,t}, s_{2,m,t}, s_{3,m,t}]$  where  $s_{1,m,t}$  and  $s_{2,m,t}$  are the AUV  $(x, y)$  planar locations, at constant altitude above the seabed, and  $s_{3,m,t}$  is its heading,  $\theta$ . For particle  $m$  at time  $t$ .

$$f_t = \begin{bmatrix} s_{1,m,t} \\ s_{2,m,t} \end{bmatrix} = \begin{bmatrix} s_{1,m,t-1} \\ s_{2,m,t-1} \end{bmatrix} + \begin{bmatrix} \cos s_{3,m,t} \\ \sin s_{3,m,t} \end{bmatrix} \times u_t \times dt + w_t \quad (5)$$

$u_t$  is the AUV constant speed,  $dt$  is the time step (0.5 minutes) and  $w_t$  is a  $2 \times 1$  matrix  $\sim N(0, Q)$  as linear Gaussian additive noise. The AUV position covariance matrix,  $Q$ , is then a  $2 \times 2$  matrix. The gravity gradient vector is defined as:

$$GG = \left[ \frac{\partial^2 G}{\partial x^2}, \frac{\partial^2 G}{\partial x \partial y}, \frac{\partial^2 G}{\partial y \partial x}, \frac{\partial^2 G}{\partial y^2} \right]. \quad (6)$$

It is numerically calculated for each of the gravimeter measurements,  $G(i,j)$ , at the prior mapped locations.

The particle filter measurement model,  $h_t$ , searches through map,  $\mathcal{M} = \{M_i, M_j\}$ , for the prior gravimeter landmark closest to the AUV position  $s_{m,t}$  within the gravimeter sensor's range. The measurement noise  $\sim N(0, R)$ . An extended Kalman filter update tries to associate this gravimeter measurement and its location with previously mapped landmarks. The association is achieved through individual compatibility then nearest neighbour. Individual compatibility rules out statistically unlikely associations based on the sum of the differences between the predicted and calculated gravity gradients i.e.:

$$\min(\sum_{i=1}^4 \|predicted(GG(i)) - mapped(GG(i))\|). \quad (7a)$$

Then, of that subset, nearest neighbour selects the best landmark based on the Mahalanobis distance:

$$mDist_i = (s_{i,m,t} - l_i)P^{-1}; d = \sqrt{\sum_{i=1}^2 \left( \frac{mDist_i}{\sigma_{landmark,i}} \right)^2}. \quad (7b)$$

If the landmark was previously observed and correctly associated, the update improves the AUV position state estimate and covariance. If the landmark was not previously observed then, its pose and covariance are augmented into the prior map as a potential map update.

The particle filter uncertainties were selected as follows. As mentioned earlier, gravimeters measurement accuracies can be  $\pm 1.0 - 2.0$  mGal. The marine gravity anomaly model used, grav.img.24.1 (Sandwell, et al., 2014), has an accuracy of  $\pm 3 - 8$  mGal. Consequently, the total measurement uncertainty is taken to be  $\pm 6$  mGal for this analysis. The AUV forward motion model uncertainty used is 1% of distance travelled and the heading measurement uncertainty is 0.1 degrees. The particle filter solutions are compared against the motion model implementation without the noise,  $w_t$ , in Eq. (5).

## 3. IMPLEMENTATION OF METHODOLOGY

Given the *a priori* marine gravimeter maps, the SLAM mission simulated is to re-acquire gravimeter landmarks. Towards

that, the first task is to define an AUV mission that clearly shows the localization limits given a variety of gravimeter map qualities. The gradients,  $GG$  from Eq. (6), derived from the gravimeter measurements were used as there are 4 gradients that could be calculated at each prior measured point. The rationale is that the more attributes that could be jointly associated with a landmark, the greater the likelihood of a successful data association. Therefore, the mission is to transit at constant heading and speed to re-acquire prior measurements. This mission geometry makes it easy to analyze and assess the particle filter SLAM performance. As well, it is easier to choose a constant heading AUV mission that might go through interesting or difficult gravity terrain. For example, a mission along a gravity anomaly isocline or one that crosses highly variable gravity terrains and boundaries. Consequently, the mission prior would be the AUV initial position at  $(X(\text{km}), Y(\text{km})) = (0, Y_0)$  at a given altitude. The mission is to survey at 90 degrees heading from that prior map position. As the mission is at constant heading, a measure of the AUV location estimation performance would be the particle filter solution's standard deviation,  $Y_\sigma$ , and mean  $Y_{mean}$ , relative to the motion model without noise on that mission.

As outlined in Section 2.2, the fitness of an area for gravity-aided inertial navigation can be quantitatively assessed through its gravitational characteristics (Eqs. (1) and (4)). This paper contrasts two different illustrative gravity terrains. One is a 'good' terrain with high characteristic values. The example used is in Fig. 1a. The 'difficult' terrain (Fig. 1b) has low characteristic values and thus its potential for gravity-aided inertial navigation and potentially, SLAM, may be marginal. Both regions are offshore of Nova Scotia:

- map 1: good: long  $\in [-56.0 - 55.7]$ , lat  $\in [11.3, 11.0]$   
 $\Gamma_k$ : mean = 7.78; std = 2.58; rms = 8.13  
 As the  $\text{rms}(\Gamma_k) < 9.3$  and  $k_{\max}(\Gamma_k) / 2 = 2.0$ , the best localization  $\sim \pm 2.0$  nm (3.7 km) (Fig. 1a)
- map 2: difficult: long  $\in [-58.3, -57.7]$ , lat  $\in [11.3, 11.0]$   
 $\Gamma_k$ : mean = 1.49, std = 0.325; rms = 2.73  
 As the  $\text{rms}(\Gamma_k) \ll 9.3$  and  $k_{\max}(\Gamma_k) / 2 = 3.0$ , the best localization  $> \pm 3.0$  nm (5.6 km) (Fig. 1b)

What would be useful is a link between a terrain's characteristic values and the particle filter parameters needed.

## 4. DISCUSSION AND RESULTS

### 4.1 Higher Spatial Density Measurements

Fig. 2 shows an isometric of the raw gravity measurements used. An interpolation obviously smooths the surface (not shown). The arithmetically interpolated surface considered is at double the prior resolution, i.e.  $0.5 \text{ nm} \times 0.5 \text{ nm}$ . While this does not actually increase the resolution, it shows what is possible by increasing the gravimeter measurement frequency through supplementing with on-board AUV measurements. For the good map, interpolation allows it to better track the mean  $Y$  value,  $Y_{mean}$ , and decreases the  $Y$  standard deviation,

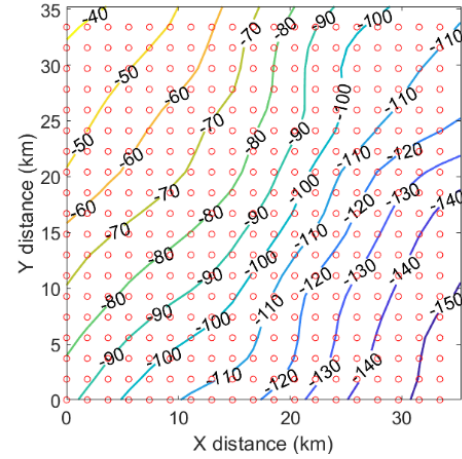


Fig. 1a: Good gravitation terrain (map 1) for gravity-aided navigation. Anomaly contour values are in mGal. Red circles are locations with prior measurements.

$Y_\sigma$ . If actual measurements were made at a higher spatial frequency their uncertainties and discontinuities would contribute errors not captured in such an interpolation. Figs. 3b and 3c show the improved mission with an increased spatial frequency in the prior anomaly measurements.

### 4.2 Analysis of Results

For good terrain, increasing the particle count yields a solution that tracks the perfect motion model better. For the configurations studied, a particle filter with 150 - 250 particles indicate whether a converged solution exists at all. If it does, then more particles refine the solution. If there is not a converged solution given 150-250 particles, then more particles will not yield a converged solution. Fig. 3a is an example of a mission with converged solution in the good map. Fig. 3b shows a converged mission in the good map that was only achievable with  $2\times$  the original prior resolution. This mission did not converge on the original prior resolution (not shown).

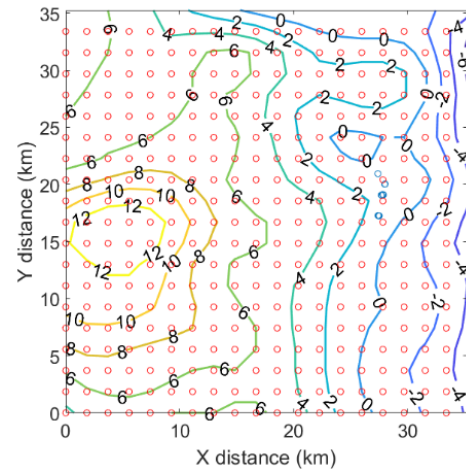


Fig. 1b: Difficult gravitation terrain (map 2) for gravity-aided navigation. Anomaly contour values are in mGal. Red circles are landmark locations.

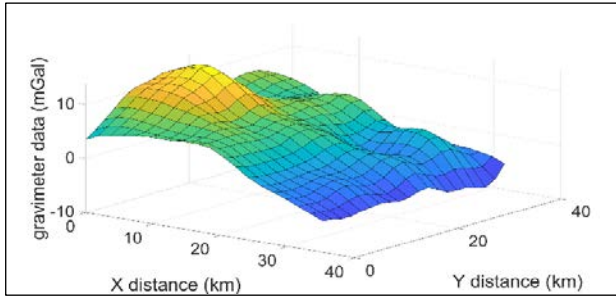


Fig. 2: Prior marine gravimeter measurements,  $G$ , used in analysis (Sandwell, et al., 2014).

The gravity anomaly characteristics captured in the standard deviation and  $\Gamma(k)$  values do not guarantee all missions within the map necessarily have a converged SLAM solution even if they are above recommended thresholds in the literature (Wang, et al., 2017a) as it is only a gross average for a map.

The higher the measurement noise  $\sim N(0, R)$  is the more difficult it is to achieve a converged solution. However, the likelihood for converged SLAM solutions is much greater in good than in difficult terrains as characterized by  $\Gamma(k)$ .

Not unexpectedly, in the case of the difficult terrain, it was generally hard to find any mission with a converged SLAM solution. Increased particle count and landmark interpolation made no difference. There can be an exceptional case even in difficult terrain where a converged solution exists. The gravitational anomaly characteristics are a macroscopic measure for an area and not representative of a local measure of SLAM fitness. This stands to reason as the gravitational anomaly measures combine navigation and localization figures of merit into one. For localization purposes, the nearfield (local) localization parameter  $\Gamma(i, j, k)$ , in Eq. (3) is a better measure of a region's potential SLAM fitness.

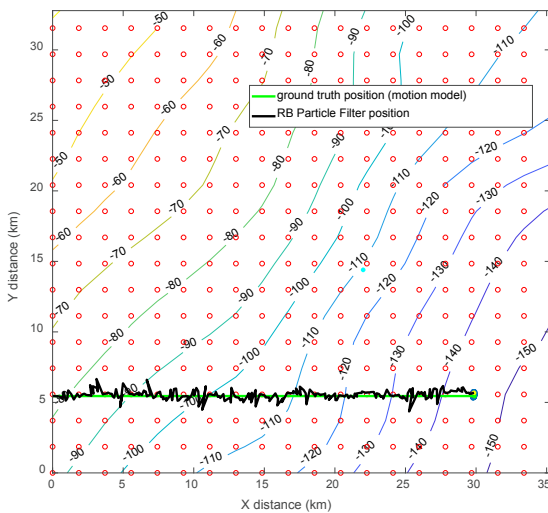


Fig. 3a: Particle filter AUV localization solution using gravimeter measurements at the prior resolution ( $1 \text{ nm} \times 1 \text{ nm}$ ) on the good map for mission  $Y_0 = 5.5 \text{ km}$ . Achieved  $Y_{\text{mean}} = 5.53$ ,  $Y_{\sigma} = 0.32 \text{ km}$ . This solution converges.

Even in a good map there can be missions that do not converge. The ones that do converge have larger variations in the adjacent landmark  $\Gamma(i, j, k)$  values around the current AUV position (Fig. 4). For the converged solution, the characteristic value has a maximum of 4.2 and minimum of 2 along the path while the diverged solution has a maximum of 3.8 and a minimum of 2.8 along the path. This shows the characteristic parameters ability to predict the performance of a localization algorithm. This is a consideration as the prior landmarks are  $1 \text{ nm}$  apart and AUV navigation solutions can diverge before that distance. Future work will explore this.

A vector field histogram approach (Borenstein & Koren, 1991), with histogram values based on the  $\Gamma(i, j, k)$  landmark values immediately around the AUV position, could be used to plan a path to a destination with less position error. This would be achieved by choosing the best adjacent landmark to for the AUV to head towards.

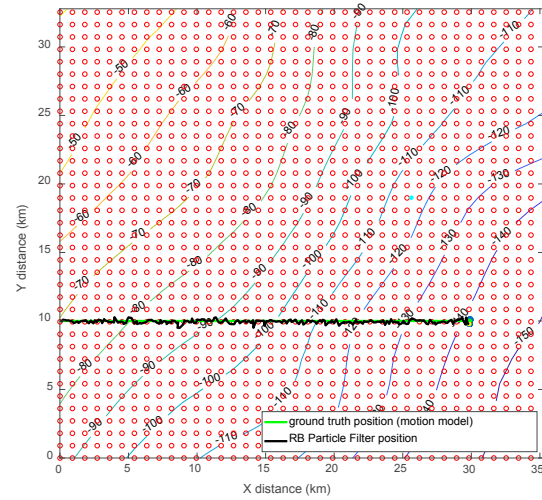


Fig. 3b: Particle filter AUV localization solution using interpolated gravimeter measurements at  $2 \times$  prior resolution ( $0.5 \text{ nm} \times 0.5 \text{ nm}$ ) on good map for mission  $Y_0 = 10 \text{ km}$ . Achieved  $Y_{\text{mean}} = 9.9$ ,  $Y_{\sigma} = 0.13 \text{ km}$ . This solution converges with this increased resolution but did not at the original prior resolution.

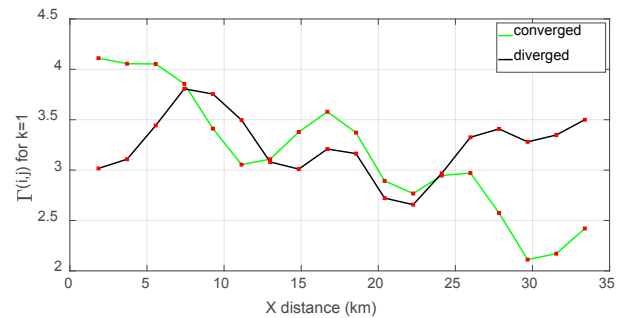


Fig. 4:  $\Gamma(i, j, k)$  for  $k=1$  with the good map for converged ( $Y_0 = 5.45 \text{ km}$ , Fig. 3a) and diverged ( $Y_0 = 10 \text{ km}$ , not shown) missions. Greater  $\Gamma(i, j, k)$  variability in converged one.



This may not guarantee a solution for the AUV to arrive at its destination in the shortest time if the AUV is surrounded by difficult local terrain. The particle filter might be able to adapt through increased particle count.

## 5. CONCLUDING REMARKS

The objective was to determine the feasibility of prior point gravity anomaly measurements for long range AUV localization potentially through SLAM. Earlier work assessed the feasibility of such measurements for gravity-aided inertial navigation by quantifying  $G$  variability over a region. At a regional level, these parameters are not revealing about potential local SLAM suitability. Characterizing the landmark-to-landmark variability in the region that the AUV transits through is a better measure of potential SLAM suitability. A viable AUV SLAM mission is one with loop-closure landmarks that are as different as possible, in magnitude, from adjacent anomaly landmarks. However, high gravitation characteristic regions require more particles in the particle filter for a converged solution.

An analysis with the interpolated anomaly measurements shows even with good gravity terrain, a  $1 \text{ nm} \times 1 \text{ nm}$  spatial frequency is difficult for accurate underwater localization. The state-of-the-art gravimeter measurement accuracies of  $\pm 2 \text{ mGal}$  mentioned earlier may be adequate for detecting ore deposits but not always so for underwater localization.

Gravity gradients derived from differencing gravity anomaly measurements appears to work for the simulations here. Actual gradiometer measurements were not used because they consist of spot measurements only. One could also supplement the potential SLAM with on-board gradiometer measurements. Compared with gravimeters, gravity gradiometers are insensitive to common-mode errors like translational acceleration, height dependence of gravity and the Eotvos effect, which will appear on an AUV. Therefore, anomalies are better suited to matching whereas gradients are more appropriate for moving platforms.

An analysis could be performed before deploying to select optimal areas and missions that the AUV could transit through to its destination position with reduced localization error. These anomaly measurements, and the tools developed here, could be applied to that step. Then, detailed gravity anomaly maps could be built in situ between the prior landmarks with the gravimeter/gradiometer-enabled AUV.

## REFERENCES

- Ander, M. E., Summers, T. & Gruchalla, M.E., 1999. LaCoste & Romberg gravity meter: System analysis and instrumental errors. *Geophysics*, Volume 64, pp. 1708-1719
- Araya, A. et al., 2015. Development and demonstration of a gravity gradiometer onboard an autonomous underwater vehicle for detecting massive seafloor deposits. *Ocean Engineering*, Volume 105, pp. 64-71.
- Barkby, S., Williams, S. B., Pizarro, O. & Jakuba, M. V., 2011. A Featureless Approach to Efficient Bathymetric SLAM Using Distributed Particle Mapping. *Field Robotics*, 28(1), pp. 19-39.
- Borenstein, J, Koren, Y., 1991. The vector field histogram – fast obstacle avoidance for mobile robots. *Transactions on Robotics and Automation*, Volume 7, pp. 278-288.
- Heath, P., Greenhalgh, S. & Direen, N. G., 2005. Modelling gravity and magnetic gradient tensor responses for exploration within the regolith. *Exploration Geophysics*, 36(4), pp. 357-364.
- Ishihara, T. et al., 2015. *Development of an Underwater Gravity Measurement System with Autonomous Underwater Vehicle for Marine Mineral Exploration*. s.l., s.n., p. 7.
- Jircitano, A., White, J. & Dosch, D., 1990. *Gravity Based Navigation of AUVs*. s.l., s.n., pp. 177-180.
- Kinsey, J., Tivey, M. A. & Yoerger, D. R., 2008. *Toward High-Spatial Resolution Gravity Surveying of the Mid-Ocean Ridges with Autonomous Underwater Vehicles*. s.l., s.n., p. 10.
- Kiselev, L., Medvedev, A. V., Kostousov, V. B. & Tarkhanov, A. E., 2017. *Autonomous Underwater Robot as an Ideal Platform for Marine Gravity Surveys*. s.l., s.n., pp. 1-4.
- Melo, J. & Matos, A., 2017. Survey on advances on terrain based navigation for autonomous underwater vehicle. *Ocean Engineering*, pp. 250-264.
- Saeedi, S., Trentini, M., Seto, M. & Li, H., 2016. Multiple-robot Simultaneous Localization and Mapping - a Review. *Field Robotics*, 33(1), pp. 3-46.
- Sandwell, D. et al., 2014. New global marine gravity model from CryoSat-2 and Jason-1 reveals buried tectonic structure.. *Science*, Volume 345, pp. 65-67.
- Shinohara, M. et al., 2017. *Mapping of Seafloor Gravity Anomalies by Underwater Gravity Measurement System Using Autonomous Underwater Vehicle for Exploration of Seafloor Deposits*. Anchorage, s.n., p. 6.
- Walcott-Bryant, A., Kaess, M., Johannsson, H. & Leonard, J. J., 2012. *Dynamic pose graph SLAM: long-term mapping in low dynamic environments*. s.l., IEEE, pp. 1871-1878.
- Wang, H. et al., 2017b. Location Accuracy of INS/Gravity-Integrated Navigation System on the Basis of Ocean Experiment and Simulation. *Sensors*, p. 13.
- Wang, H. et al., 2016. Technology of gravity aided inertial navigation system and its trial in South China Sea. *IET Radar, Sonar and Navigation*, 10(5), pp. 862-869.
- Wang, H. et al., 2017a. Characteristics of Marine Gravity Anomaly Reference Maps and Accuracy Analysis of Gravity Matching-Aided Navigation. *Sensors*, p. 14.
- Wu, L., Ma, J. & Tian, J., 2010. *A Self-adaptive Unscented Kalman Filtering for Underwater Gravity Aided Navigation*. s.l., IEEE, pp. 142-145.
- Yan, Z., Tian, J., Ma, J. & Zhang, W., 2014. *Modelling Local Gravity Anomaly Self-Adaption Quotient Reference Maps for Underwater Autonomous Navigation*. s.l., IEEE, pp. 945-949.